Journal of Integrative Agriculture 2026, 25(8): 3341–3351

Available online at ScienceDirect

Journal of Integrative Agriculture



RESEARCH ARTICLE

Discovery of N-phenyl-isoindole-1,3-dione derivatives as potent insect chitinase O*f*Chi-h inhibitors through virtual screening

Jiahao Zhang[1], Shenmeng Bai[1], Jiaxin Chu[1], Baokang Ding[1], Bohou Li[1], Yanzhu Li[1], Jingwen Guo[1], Fengyue Suo[1], Shujie Ma[1], Jingao Dong[1], Lihui Zhang[1#], Shengqiang Shen[1, 2#], Lili Dong[1#]

[1] *College of Plant Protection/State Key Laboratory of North China Crop Improvement and Regulation, Hebei Agricultural University, Baoding 071001, China*

[2] *Exosome Origin (Zhejiang) Technology Co., Ltd., Wenzhou 325024, China*

Highlights

- A novel class of N-phenyl-isoindole-1,3-dione (**PI**) derivatives was identified as potent inhibitors of O*f*Chi-h *via* virtual screening. Compound **PI-17** demonstrated strong inhibitory activity against O*f*Chi-h (K_i=2.3 μmol L^{-1}) and superior insecticidal efficacy against *Ostrinia furnacalis*.
- **PI**-series induced morphological aberrations in the cuticles of *O. furnacalis* larvae. The mechanism of this efficient insecticidal action was elucidated at atomic and electronic levels through electrostatic potential (ESP) and density functional theory (DFT) analyses.
- **PI**-series compounds demonstrated significant potential as eco-friendly insect growth regulators, with comprehensive safety assessments confirming minimal effects on natural enemies and non-target organisms.

Abstract

Ostrinia furnacalis represents a destructive lepidopteran pest causing up to 30% yield losses in maize crops globally. Its larvae penetrate plant tissues, disrupt nutrient transport, and transmit viral and microbial pathogens, exacerbating food security concerns. Current management approaches for *O. furnacalis* primarily rely on synthetic pesticides. Targeting chitin metabolism presents a promising strategy for green insecticide development. Specifically, O*f*Chi-h, an essential chitinase for *O. furnacalis* molting and survival, has emerged as a viable target. This study identified a N-phenyl-isoindole-1,3-dione (**PI**) scaffold as a novel class of O*f*Chi-h inhibitor through virtual screening strategy. Notably, compound **PI-17** demonstrated potent inhibitory activity against O*f*Chi-h with a K_i value of 2.3 μmol L^{-1}. **PI-17** exhibited significant insecticidal activity against lepidopteran pests *O. furnacalis*, comparable to the control drug hexaflumuron. Scanning electron microscopy (SEM) analysis revealed morphological alterations in the cuticles of *O. furnacalis* larvae treated with **PI**-series compounds. Electrostatic potential (ESP) and density functional theory (DFT) calculations explored the variations in biological activities of the **PI**-series compounds at atomic and electronic levels. Additionally, comprehensive safety evaluations assessed the impact on the natural enemy *Trichogramma ostriniae* and nontarget organisms. These findings introduce a novel class of lead compounds, **PI** derivatives, showing significant potential for developing eco-friendly insect growth regulators to control *O. furnacalis*.

Keywords: insect growth regulators, chitinase inhibitors, O*f*Chi-h, N-phenyl-isoindole-1,3-dione, virtual screening

1. Introduction

The *Ostrinia furnacalis*, a destructive lepidopteran pest, causes extensive damage to maize crops worldwide (Taddele *et al.* 2023). The larvae of *O. furnacalis* penetrate maize stalks, ears, and leaves, impeding nutrient transport, compromising plant structural integrity, and reducing yield by up to 30% during severe infestations (Guo *et al.* 2022; Wang *et al.* 2024). Additionally, *O. furnacalis* larvae facilitate

Received 23 May 2025; Received in revised form 1 July 2025; Accepted 13 July 2025; Available online 21 August 2025
[#]Correspondence Lili Dong, Tel: +86-312-7520235, E-mail: lilidong@hebau.edu.cn; Shengqiang Shen, E-mail: shenshengqiang@pku.edu.cn; Lihui Zhang, E-mail: zhanglihui@hebau. edu.cn

© 2026 CAAS. Publishing services by Elsevier B.V. on behalf of KeAi Communications Co. Ltd. This is an open access article under the CC BY-NC-ND license (http://creativecommons.org/licenses/by-nc-nd/4.0/). Peer review under responsibility of Editorial Board of *Journal of Integrative Agriculture*.
doi: 10.1016/j.jia.2025.08.019

the introduction of viral and microbial pathogens into plants during inflorescence feeding, leading to fruit contamination and the spread of diseases such as maize streak virus and maize dwarf mosaic virus (Monjane *et al.* 2020; Luo *et al.* 2021). This pathogen transmission intensifies food security concerns by increasing yield losses and degrading crop quality (Deng *et al.* 2023; Fan *et al.* 2024). Contemporary management approaches for *O. furnacalis* primarily depend on synthetic pyrethroids and neonicotinoids; however, extensive application has resulted in resistant populations emerging across multiple regions (Perry and Moschini 2020; Sun *et al.* 2022; Wang *et al.* 2023; Ge *et al.* 2025). Biological control methods, including natural enemy utilization and genetically modified crops expressing insecticidal proteins, present alternatives but face limitations such as restricted pest spectra or societal concerns (Zhang *et al.* 2018; Cui *et al.* 2020; Li *et al.* 2022). Consequently, developing novel, environmentally sustainable, and effective strategies to control *O. furnacalis* remains imperative.

Chitin, a linear polysaccharide consisting of β-(1,4)-linked-N-acetylglucosamine units, functions as an essential structural component of the insect exoskeleton and peritrophic matrix (Zhang *et al.* 2021). As chitin is not present in mammals and higher plants, targeting its metabolic pathways presents a promising approach for developing eco-friendly insecticides (Dong *et al.* 2021; Zhou *et al.* 2025). Among these pathways, the chitinase O*f*Chi-h, a critical enzyme responsible for chitin degradation in *O. furnacalis*, has attracted considerable attention due to its exclusive presence in lepidopteran insects (Chen *et al.* 2014; Han *et al.* 2022). O*f*Chi-h effectively hydrolyzes glycosidic bonds of chitin chains from the reducing end, serving a crucial function in insect molting, metamorphosis, and survival (Ding *et al.* 2023a).

Chitinase O*f*Chi-h inhibitors, compounds that block the catalytic activity of the enzyme, present a promising strategy for pest management. Several O*f*Chi-h inhibitors have been documented, including TMG-$(GlcNAc)_4$ (Liu *et al.* 2017), Phlegmacin B_1 (Chen *et al.* 2017), Berberines (Duan *et al.* 2018), Deoxyshikonin (Li *et al.* 2021), Polonimides and Lynamicin B (Lu *et al.* 2021), Azo-aminopyrimidines (Ding *et al.* 2025), Dipyrido-pyrimidines (Jiang *et al.* 2020), Naphthylamides (Shen *et al.* 2019; Liang *et al.* 2024), Triazolo-quinazolinones (Dong *et al.* 2023), Rhodanines (Han *et al.* 2023), SN-38 (Ding *et al.* 2023b), Guanidines (Zhao *et al.* 2023), Thiazolylhydrazones (Yang *et al.* 2020). Small-molecule inhibitors developed through rational design and natural product exploration demonstrate potent inhibitory effects against *Of*Chi-h *in vitro* (Zou *et al.* 2024). Nevertheless, significant challenges persist, including limited bioavailability, synthesis complexity, and the requirement for extensive optimization to achieve an optimal balance between efficacy and toxicity (Li *et al.* 2021). Despite these limitations, the potential application of chitinase inhibitors as environmentally friendly pesticides underscores the necessity for continued research in this field (Chen and Yang 2020).

Virtual screening, an *in-silico* methodology that computationally evaluates large compound libraries to identify potential candidates with desired biological activities, has significantly enhanced the drug discovery process (Ece 2023; Maddeboina *et al.* 2024; Niazi and Mariam 2024). Considering the essential role of O*f*Chi-h in the life cycle of *O. furnacalis* and the constraints of current chitinase inhibitors, virtual screening targeting O*f*Chi-h remains highly relevant. This study implements a virtual screening approach to identify novel O*f*Chi-h inhibitors containing an N-phenyl-isoindole-1,3-dione (**PI**) scaffold. Among these compounds, **PI-17** emerged as a potent O*f*Chi-h inhibitor with a K_i value of 2.3 μmol L^{-1}. Furthermore, **PI-17** demonstrated superior insecticidal activity against *O. furnacalis* compared to the insecticide hexaflumuron. These findings reveal a novel class of lead compounds with substantial potential for developing agricultural pest control agents.

2. Materials and methods

2.1. Chemical-database preparation

The SPECS database, comprising 200 thousand well-characterized small molecules, was utilized for virtual screening to identify potential candidates. The compounds were downloaded and processed using the CONCORD module of Sybyl 7.3, which transforms the 2D molecular structures into 3D conformations. These processed compounds were subsequently employed for virtual screening analyses.

2.2. Virtual screening

The cocrystal structure of O*f*Chi-h with its bound ligand dipyrido-pyrimidine (PDB ID:6JMN) served as a template for molecular docking. The *Structure Preparation* function in Molecular Operating Environment (MOE) software was utilized to preprocess the protein structures. This preprocessing included evaluating protein-structure data quality based on temperature factors, performing protein geometry and electron-density checks, adding hydrogen atoms with optimized positions, and conducting final energy minimization. To identify high-quality candidate inhibitors, two molecular docking algorithms — Surflex Deck GeomX mode and MOE docking program — were independently employed for docking-based virtual screening. The initial virtual screening utilized the Surflex-Dock GeomX program within the Sybyl 7.3 software suite in ligand mode. The docking process considered molecular ring flexibility, retaining 20 conformations per molecule for scoring using an empirically derived function. For MOE docking, ligand poses were generated and their binding free energy estimated using the Triangle Matcher placement algorithm and London dG scoring function. The Rigid Receptor protocol with GBVI/WSA dG was applied to refine pose placement and score each generated pose, maintaining 20 conformations per molecule for final evaluation. The hits were subsequently ranked by docking scores from lowest to highest. After comprehensive analysis, the top 100 compounds scoring highly in both functions were selected. Candidates were filtered through visual analysis of interactions with key residues (W532, R439, W389 and W268). Ultimately, 15 compounds were procured from Shanghai Topscience Corporation (China) for biological evaluation.

2.3. Enzymatic assay

The O*f*Chi-h was provided by Professor Qing Yang (Institute of Plant Protection, Chinese Academy of Agricultural Sciences). Enzymatic activity was measured using 4-methylumbelliferyl-N, N′-diacetyl-β-D-chitobioside (4-MU-$(GlcNAc)_2$, Sigma, Shanghai, China) as the substrate. The reaction mixture for inhibitor screening was conducted in a 100 μL volume containing 20 mmol L^{-1} sodium phosphate buffer (pH 6.0), O*f*Chi-h enzyme (10 nmol L^{-1}), 2% (v/v) DMSO, 4-MU-$(GlcNAc)_2$ substrate (4 μmol L^{-1}), and inhibitor. Following 20 min incubation at 30°C, the reaction was stopped by adding Na_2CO_3 solution (100 μL, 0.5 mol L^{-1}). Fluorescence intensity was measured using a microplate reader at excitation and emission wavelengths of 355 and 450 nm. All experiments were conducted in triplicate unless specified otherwise. The inhibition constant (K_i) was determined using Dixon plots by varying substrate concentration at constant concentrations (20, 10 and 5 μmol L^{-1}).

2.4. Molecular docking

Molecular docking was conducted to predict protein-inhibitor binding modes. The O*f*Chi-h-dipyridopyrimidine complex (PDB ID: 6JMN) served as the docking template. The protein structure underwent preparation in MOE *via Structure Preparation*, including geometry/electron density checks, hydrogen addition, and energy minimization. Subsequently, **PI-13** and **PI-17** were docked into the *Of*Chi-h active site using MOE's docking module. A collection of docking poses was generated using the Triangle Matcher method. The generalized-Born/volume-integral implicit-solvent model was employed to score each generated pose.

2.5. Insecticidal activity assay

The target compounds underwent testing for insecticidal activity against *Plutella xylostella* and *O. furnacalis* using the leaf dipping method. Third-instar larvae were utilized for the assay, with test compounds diluted to final concentrations of 500 and 200 μg mL^{-1} as required. The larvae were maintained at 26–28°C with 70% relative humidity. Hexaflumuron served as a positive control. Larvae underwent treatment for 4 days. Mortality was determined based on the following criterion: larvae were considered deceased when showing no response to gentle physical stimulation and inability to crawl normally. Each experimental group contained 10 larvae, with treatments performed in triplicate.

2.6 Growth regulating effects on *O. furnacalis*

The *O. furnacalis* larvae were maintained at 26°C–28°C, 70% relative humidity, with a photoperiod of 16 h light and 8 h darkness. The representative compounds were dissolved in DMSO and diluted with an artificial diet to final concentrations of 10 μmol L^{-1}. Third-instar larvae were selected for the feeding experiments. Control larvae received diets containing an equivalent amount of DMSO. Each experimental group comprised 15 individual larvae that were continuously fed for 6 days. The length and weight of each larva were measured and documented.

2.7. Scanning electron microscopy (SEM) assay

Morphological changes in the cuticle of *O. furnacalis* were examined by SEM. The *O. furnacalis* larvae were initially fixed in 2.5% glutaraldehyde at 4°C overnight. Subsequently, the samples were rinsed with 0.1 mol L^{-1} phosphate buffer for 3 h and fixed with 2% osmium tetroxide for 2 h. Following triple-washing with distilled water, the specimens underwent dehydration through a graded ethanol series (30, 50, 60, 70, 80, 90, 95, and 100% ethanol), and subjected to critical point drying. The samples were then coated with gold. Finally, the specimens were examined using a Phenom Pro scanning electron microscope at an accelerating voltage of 15 kV and a 4 mm working distance.

2.8. Electrostatic potential (ESP) and density functional theory (DFT) calculations

The energy minimization of the representative compounds was performed using Gaussian 16. In Gaussian 16, DFT and ESP calculations were conducted using the DFT-B3LYP functional with the standard 6–31+G (d, p) basis set. The ESP representations of the compounds were visualized through GaussView. The electrostatic potential surface displays a color gradient from red (most negative potential) to blue (most positive potential).

2.9. Effect of the target compounds on *Trichogramma ostriniae*

The acute toxicity of target compounds to *T. ostriniae* was evaluated using the dry film residual contact method. The compounds dissolved in ethanol (100 μL of 0.5 mg mL^{-1}) were introduced into a 10 mL centrifuge tube with a lid (82 mm×15.4 mm). The tube was rotated to ensure uniform coating of the solution on the inner wall. For the control group, 100 μL of ethanol was added to the centrifuge tube. After complete ethanol evaporation, 100±10 adult *T. ostriniae* aged 4 to 6 h were introduced. After 8 h, the adult insects were counted to calculate the survival rate. Additionally, the effect of the compounds on *T. ostriniae* egg hatching was assessed. Cards carrying eggs (100±20) of *T. ostriniae* were immersed in a compound solution at 500 mg L^{-1}. The naturally dried oocytes at 25°C were carefully placed into a clean centrifuge tube. Ethanol served as the negative control. After 48 h, the hatching rate of *T. ostriniae* eggs was recorded.

2.10 Biosafety prediction

To investigate the biosafety of the target compounds towards non-target organisms, carcinogenicity and bee toxicity predictions were conducted using Toxtree-v3.1.0 (http://toxtree.sourceforge.net) and admetSAR (http://lmmd.ecust.edu.cn/admetsar2). The cytotoxicity assessment was performed *via* MouseTox (https://comptox.epa.gov/dashboard/predictions), a specialized platform for predicting molecular cytotoxicity on NIH/3T3 cells. The toxicity estimation software tool (T.E.S.T., version 5.1.2), developed by the US Environmental Protection Agency (EPA), was utilized to predict the oral median lethal dose (LD_{50}) in rats. The toxicity grades were analyzed according to US EPA

pesticide toxicity categorization standards. Compounds with an LD_{50} below 50 mg kg^{-1} are classified as highly toxic, those with an LD_{50} between 50 and 500 mg kg^{-1} as moderately toxic, compounds with an LD_{50} between 500 and 5,000 mg kg^{-1} as less toxic, and substances with an LD_{50} exceeding 5,000 mg kg^{-1} as slightly toxic.

3. Results

3.1. Novel O*f*Chi-h inhibitors obtained by virtual screening

The SPECS database, containing 200,000 molecules, was utilized for virtual screening. The crystal structure of O*f*Chi-h complexed with dipyrido-pyrimidine (PDB ID: 6JMN) served as the docking template. To enhance the accuracy of virtual screening based on molecular docking, a parallel screening strategy was implemented, independently docking the database molecules using both the Surflex-Dock GeomX program in Sybyl and MOE modeling software. The initial screening was conducted using Surflex-Dock GeomX in Sybyl 7.3, employing a cutoff score of 7.5 (dipyrido-pyrimidine ligand showed a docking score of 9.2), yielding the top 2,000 compounds. Given the different scoring algorithms between Sybyl 7.3 and MOE software, the DOCK module in MOE was applied in parallel, using a critical score of 7.0 (docking score of 9.1 for dipyrido-pyrimidine ligands), identifying another top 2,000 compounds. Through comprehensive analysis, the top 100 compounds ranked in both scoring functions were identified. These hits underwent further refinement through visual analysis. Based on key interactions in O*f*Chi-h-inhibitor crystal complexes, particular attention was paid to interactions between compounds and residues W532, R439, W389 and W268. The top 15 ranked compounds were subsequently procured from Shanghai Topscience Corporation (China) for biological evaluation. The structures and inhibition rates of these compounds are presented in Appendix A.

As detailed in Appendix A, compound **VSIII-6** (**PI-1**) demonstrated exceptional inhibitory activity against O*f*Chi-h with an inhibition rate of 81.6% at 20 μmol L^{-1}. Three compounds, **VSIII-5**, **VSIII-7**, and **VSIII-10**, exhibited significant activity against O*f*Chi-h with inhibition rates exceeding 65%. These results validate the effectiveness of the virtual screening approach. Subsequent enzyme inhibition assays determined the IC_{50} of **PI-1** against O*f*Chi-h to be 10.7 μmol L^{-1}. Compound **PI-1**, containing an **PI** structure, represents a novel and streamlined scaffold previously unreported for chitinase inhibition. These characteristics of **PI-1** correspond well with the study's established criteria, establishing it as a promising candidate for further structural modification.

3.2. Structural modification of PI-1

To develop compounds with improved inhibitory activity against O*f*Chi-h, **PI-1** was selected as the lead compound for structural modification. Through structural similarity analysis in the SPECS database, a series of phenyl-isoindole-1,3-dione compounds **PI-2-10** were identified and obtained (Fig. 1-A and Table 1). The inhibitory activity of these compounds against O*f*Chi-h was evaluated at 10 μmol L^{-1}.

As shown in Table 1, most compounds demonstrated enhanced inhibitory potency compared to the initial compound **PI-1**. Evaluation of **PI-1-6** (with identical substituents at R_2, R_3, and R_4 positions) for inhibitory potency against O*f*Chi-h revealed that R_1 position substituents significantly influenced efficiency. The inhibitory activity increased with larger halogen substituents (F, Cl, and Br) at the 4-position on the benzene ring (compounds **PI-2**<**PI-1**<**PI-3**). This suggests that the 4-substituent size may be the primary factor affecting inhibitory activity. Shifting the 4-Cl group of **PI-1** to 2-Cl (**PI**-1 to 2-Cl (**PI-4**)) decreased inhibitory potency. At the 3-position of the benzene ring, strong electron-withdrawing substituents like the nitro group enhanced activity more effectively than electron-donating groups such as the methoxy group (**PI-5**>**PI-6**). Additionally, introducing a 2-hydroxy substitution on the benzene ring at the R_2 position substantially reduced the inhibitory effect (**PI-7**<**PI-2**, **PI-8**<**PI-3**). Moreover, adding a methyl substituent at the R_4 position decreased activity (**PI-9**<**PI-1**). Conversely, incorporating a methyl group at the R_3 position markedly enhanced inhibitory efficiency (**PI-10**>**PI-1**). The preliminary structure-activity relationships (SARs) indicate that activity against O*f*Chi-h is enhanced by: a large halogen substituent at the 4-position of R_1 (such as 4-Br), an electron-withdrawing group at the 3-position of R_1 (such as 3-NO_2), and an appropriately sized hydrophobic moiety at the R_3 position (such as CH_3).

3.3. Further optimization of PI derivatives

Building upon the preliminary SARs studies, further structural optimization of the **PI**-series compounds was conducted. A methyl group was fixed at the R_3 position while investigating how substituent changes at the R_1 position affected inhibitory

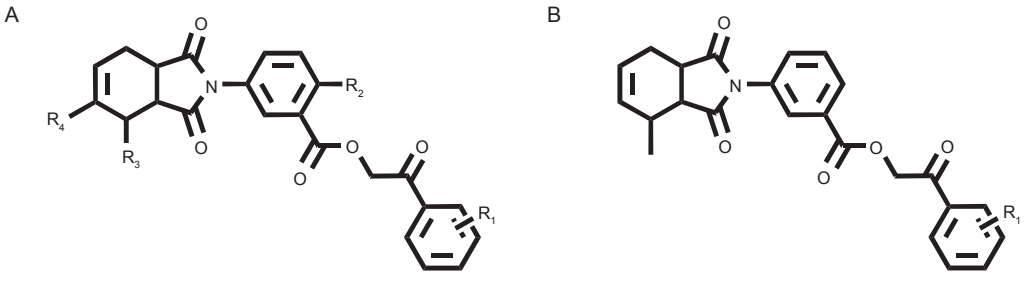


Fig. 1 Chemical structural skeleton of N-phenyl-isoindole-1,3-dione (PI) derivatives. A, chemical structure skeleton and substituent distributions of **PI-1** to **PI-10**. B, chemical structure skeleton and substituent distributions of **PI-11** to **PI-17**.

Table 1 Inhibitory activity of compounds PI-1-10 against O*f*Chi-h

Compound	Substituent group				Inhibition rate at 10 μmol L^{-1} (%)	IC_{50} values (μmol L^{-1})
	R_1	R_2	R_3	R_4		
PI-1 (VSIII-6)	4-Cl	H	H	H	51.6±8.5	10.7±0.4
PI-2	4-F	H	H	H	44.9±1.4	–
PI-3	4-Br	H	H	H	66.5±4.9	7.3±0.2
PI-4	2-Cl	H	H	H	33.9±2.6	–
PI-5	3-NO_2	H	H	H	68.6±3.5	5.4±0.2
PI-6	3-OCH_3	H	H	H	48.3±4.8	–
PI-7	4-F	OH	H	H	39.2±7.5	–
PI-8	4-Br	OH	H	H	61.8±5.4	7.6±0.3
PI-9	4-Cl	H	H	CH_3	31.5±3.1	–
PI-10	4-Cl	H	CH_3	H	75.4±1.0	3.8±0.1

– indicates not determined (less than 50% inhibition at 10 μmol L^{-1}).

Table 2 Inhibitory activity of compounds PI-11-17 against O*f*Chi-h

Compound	Substituent group	Inhibition rate at 5 μmol L^{-1} (%)	IC_{50} values (μmol L^{-1})
	R_1		
PI-11	4-H	10.3±5.7	–
PI-12	4-CH_3	24.6±5.5	–
PI-13	4-Br	73.0±1.0	2.6±0.3
PI-14	4-OCH_3	62.1±7.6	3.8±0.6
PI-15	3, 4-di-CH_3	52.7±7.4	6.0±0.5
PI-16	3-NO_2-4-CH_3	65.4±4.1	3.8±0.1
PI-17	3-NO_2-4-Cl	67.6±2.5	3.1±0.7

– indicates not determined (less than 50% inhibition at 5 μmol L^{-1}).

activity (Fig. 1-B and Table 2). Electron-withdrawing groups at the 4-position of the benzene ring proved more effective than electron-donating groups in enhancing inhibitory activity (**PI-13**>**PI-11**, **PI-12** and **PI-14**). The nitro group at the 3-position of the benzene ring remained essential for increasing potency (potency (**PI-16**) and **PI-17**>**PI-15**). IC_{50} determination revealed that **PI-13** and **PI-17** exhibited the highest efficiency against O*f*Chi-h among compounds **PI-1-17**, with IC_{50} values of 2.6 and 3.1 μmol L^{-1}, respectively.

3.4. Inhibitory mechanism

To elucidate the inhibitory mechanism of the **PI**-series compounds, representative inhibitors **PI-13** and **PI-17** were selected for inhibition constant (K_i) analysis using Dixon plots approach. As illustrated in Fig. 2, **PI-13** and **PI-17** demonstrated competitive inhibition toward O*f*Chi-h, evidenced by the intersection of substrate concentration trendlines in quadrant two. The K_i values for **PI-13** and **PI-17** against O*f*Chi-h were determined to be (3.0±0.3) and (2.3±0.1) μmol L^{-1}, respectively.

To elucidate the mechanistic basis for the potency of these O*f*Chi-h inhibitors, molecular docking studies revealed the binding modes of compounds **PI-1**, **PI-13**, and **PI-17** with O*f*Chi-h. The conformations of inhibitors **PI-1**, **PI-13**, and **PI-17** in the active pocket of O*f*Chi-h were analyzed as shown in Fig. 3. The conformations of **PI-13** and **PI-17** demonstrate similar binding patterns in the O*f*Chi-h pocket, primarily interacting at the –2, –1, +1, and +2 subsites. The N-phenyl and isoindole-1,3-dione moieties of these inhibitors bound to the +1 and +2 subsite, while the side chain phenyl fragment bound to the –2 subsite. In contrast, the isoindole-1,3-dione fragment of **PI-1** occupies the –1 and –2 subsites of O*f*Chi-h, with the side chain phenyl portion binding to the +2 subsite (Fig. 3-A).

Specifically, the N-phenyl isoindole-1,3-dione moiety of **PI-1** interacts with residues W532, W268, and R439 *via* strong π-π stacking and hydrogen bonding interactions. The side chain of the *p*-methoxyphenyl ring, positioned at the entrance of the active pocket, forms interactions with residues W389, F385 and M381 (Fig. 3-B). These binding interactions align with the crystallographic observations in the O*f*Chi-h-dipyridopyrimidine complex (PDB ID:6JMN). The methyl group on the isoindole ring of **PI-13** appears to create

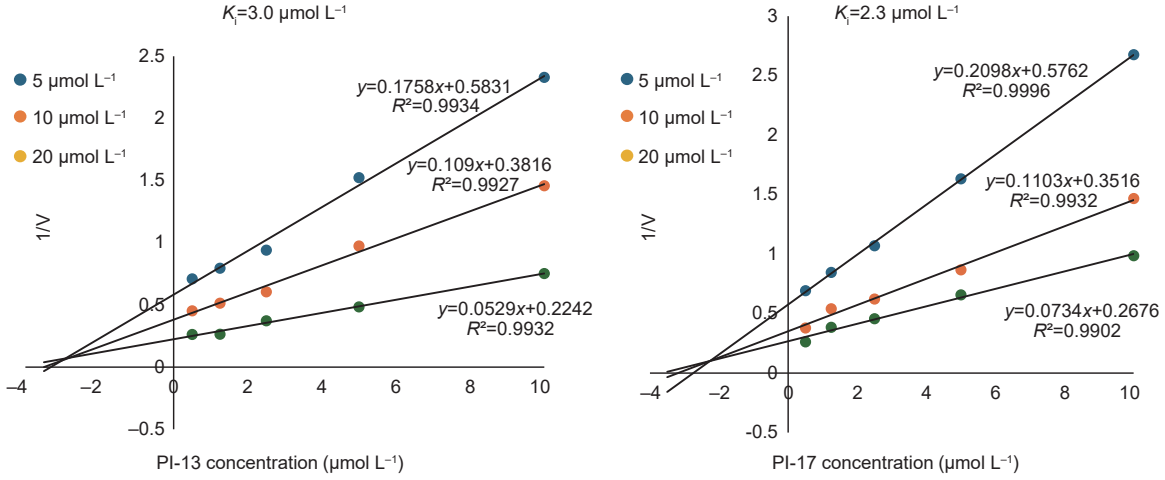


Fig. 2 Dixon plots illustrating the inhibitory effects of PI-13 and PI-17 against O*f*Chi-h. 1/V represents the reciprocal of the enzymatic reaction rate.

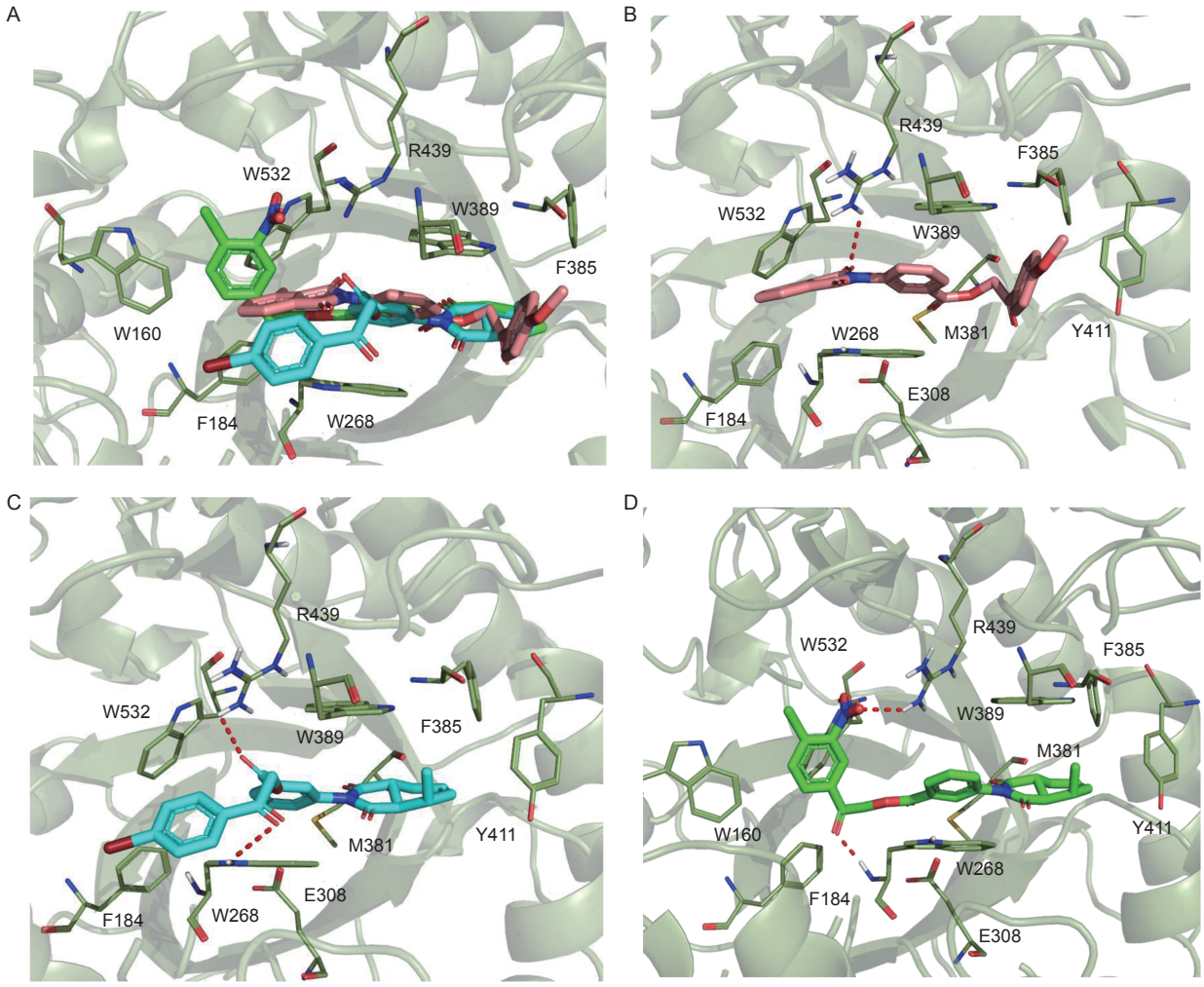


Fig. 3 Predicted binding modes of PI-1, PI-13, and PI-17 with O*f*Chi-h. A, superimposition of **PI-1**, **PI-13**, and **PI-17** in the O*f*Chi-h binding pocket. B–D, detailed binding modes of **PI-1**-O*f*Chi-h (B), **PI-13**-O*f*Chi-h (C), and **PI-17**-O*f*Chi-h (D). The O*f*Chi-h structure is represented in cartoon style. Compound **PI-1** is depicted in light pink, **PI-13** in cyan, and **PI-17** in green (colored according to atomic elements).

steric hindrance, preventing the N-phenyl isoindole-1,3-dione fragment from accessing the –1 and –2 subsites of the enzyme. Consequently, it binds to residues at the +1 and +2 subsites near the active pocket entrance. The *p*-bromophenyl fragment of the side-chain structure advantageously penetrates the –1 and –2 subsites of the pocket. Its carbonyl groups' oxygen atoms form hydrogen bonds with residues R439 and W268, respectively (Fig. 3-C). Similar interactions characterize **PI-17**. However, the 3-nitrobenzene fragment forms distinctive strong hydrogen bonding and π-π stacking interactions with R439 and W532 (Fig. 3-D), potentially explaining **PI-17**'s enhanced inhibitory activity against O*f*Chi-h.

3.5. Effects of compounds PI-13 and PI-17 on the growth of O. *furnacalis* larvae

The effects of potent inhibitors **PI-13** and **PI-17** on *O. furnacalis* larvae growth were evaluated at 10 μmol L^{-1} concentration. The compounds were administered to third-instar larvae for 6 days. As illustrated in Fig. 4-A and B, the treated group exhibited significant reductions in both body weight and length compared to the control group. Larvae treated with compound **PI-13** showed notable decreases in relative weight (27%) and body length (22%). Similarly, larvae exposed to compound **PI-17** demonstrated weight and body length reductions of 33 and 23%, respectively. After 6 days of exposure to **PI-13** and **PI-17**, the larvae exhibited symptoms including curling, reduced mobility, and diminished response to external stimuli (Fig. 4-C). These results demonstrate that N-phenyl isoindole-1,3-dione derivatives substantially inhibit the growth and development of *O. furnacalis* larvae.

To evaluate the effects of inhibitors **PI-13** and **PI-17** on the cuticle of *O. furnacalis* larvae, SEM analysis was conducted. As illustrated in Fig. 4-D, larvae exposed to compounds **PI-13** and **PI-17** demonstrated significant morphological changes in their cuticles compared to the CK. In the control group, the larval cuticle appeared smooth without irregular wrinkles, and regular chitin particles were clearly visible. However, in the experimental groups treated with **PI-13** and **PI-17**, distinct wrinkles emerged on the dorsal surfaces of the larvae. Furthermore, the chitin in the larval cuticles displayed protruding particles, increased size, and a more densely

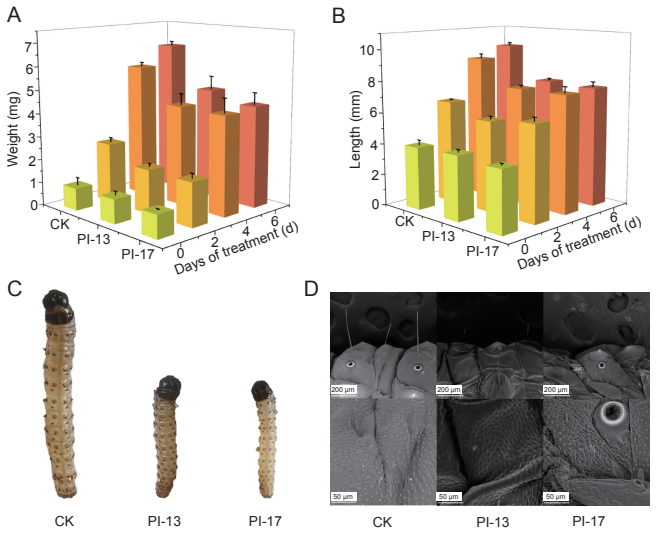


Fig. 4 Effects on the growth of *Ostrinia furnacalis* larvae treated with PI-13 and PI-17. A and B, variations in mean larval body weight (A) and body length (B) throughout the 6-day cultivation period. C, morphological alterations of *O. furnacalis* larvae. D, scanning electron microscopy (SEM) analysis of the larval cuticle of *O. furnacalis* following dietary exposure. CK, control.

packed, irregular arrangement. These observations suggest that the **PI**-series compounds effectively hydrolyze cuticular chitin, with their enzyme inhibitory capacity directly correlating to chitin molting inhibition. These findings provide preliminary but significant insights into the compounds' insecticidal mechanisms.

3.6. Insecticidal activity

The insecticidal activity of **PI**-series compounds was evaluated against lepidoptera agricultural pests *O. furnacalis* and *P. xylostella*. At 500 mg L^{-1}, most compounds demonstrated substantial insecticidal activity, achieving mortality rates of up to 100% (Table 3). At a reduced concentration of 200 mg L^{-1}, **PI-1-17** maintained mortality rates exceeding 50% against *P. xylostella*. Against *O. furnacalis*, compounds **PI-13** and **PI-16** exhibited superior activity with mortality rates exceeding 70% at 200 mg L^{-1}, surpassing the control drug hexaflumuron (66.7%). For *P. xylostella*, compounds **PI-6**, **PI-9**, **PI-10**, **PI-13**, and **PI-16** demonstrated high efficacy with mortality rates above 90% at 200 mg L^{-1}, exceeding the control drug's performance. Notably, the potent O*f*Chi-h inhibitors **PI-13**, **PI-16**, and **PI-17** demonstrated effective insecticidal activity against both species. The preliminary SARs indicate that the methyl group at the R_3 position of the isoindole ring enhances potency (**PI-9**, **PI-11-17**). Additionally, incorporating a nitro group at the 3-position (**PI-16** and **PI-17**) and a larger halogen substituent at the 4-position (**PI-9-10**, **PI-13**, and **PI-17**) of the benzene ring in R_1 group improves insecticidal activity.

3.7. ESP and DFT analysis

To elucidate the variations in biological activities of the **PI**-series compounds at atomic and electronic levels, as depicted in Fig. 5, compounds **PI-11** and **PI-13** were selected for ESP and DFT calculation analyses.

As illustrated in Fig. 5-A, the conformations of the N-phenyl isoindole-1,3-dione (**PI**) backbone of **PI-11** and **PI-13** exhibit subtle structural variations. The incorporation of a bromine atom into the benzoyl side chain of **PI-13** generates significant positive charges in the **PI** position. These negatively charged regions potentially function as bioactive centers, facilitating interactions with amino acid residues within the protein pockets. Additionally, the benzoyl side chains of **PI**-series compounds generate strong negative charges **(**Fig. 5-A). The negatively charged benzoyl moiety of **PI-11** and **PI-13** interacts with the positively charged region in the O*f*Chi-h pocket, formed by R439, W268 and W532 (Fig. 3-C). The bromine substitution in **PI-13** orients its benzoyl side chain more optimally toward the enzyme's positively charged binding site, enabling additional hydrogen bonding with R439 and W268 (Fig. 3-C). This structural modification provides **PI-13** with enhanced electrostatic complementarity compared to **PI-11**.

According to molecular orbital theory, the lowest unoccupied molecular orbital (LUMO) and the highest occupied molecular orbital (HOMO) play crucial roles in determining the biological activities of agrochemicals. The HOMO energy (E_{HOMO}) measures electron-donating capacity, with higher values indicating greater electron release potential. Conversely, the LUMO energy (E_{LUMO}) indicates electron-accepting capability, where lower values correspond to increased electrophilicity. The energy gap (ΔE) between HOMO and LUMO serves as a predictive indicator for bioactivity, with smaller energy gaps (Δ*E*) generally correlating with enhanced biological performance of agrochemicals. The LUMO and HOMO for **PI-11** primarily concentrate on its benzoyl side chain and **PI** backbone, respectively. In contrast, the LUMO and HOMO of **PI-13**, which demonstrates superior biological activity, predominantly

Table 3 Insecticidal activities (%) of compounds PI-1-17

Compound	*Ostrinia furnacalis*		*Plutella xylostella*	
	500 mg L^{-1}	200 mg L^{-1}	500 mg L^{-1}	200 mg L^{-1}
PI-1	100±0.0	56.7±4.7	100.0±0.0	66.7±11.5
PI-2	100±0.0	33.3±12.4	100.0±0.0	66.7±5.8
PI-3	100±0.0	43.3±4.7	100.0±0.0	83.3±11.5
PI-4	76.7±4.7	46.7±4.7	80.0±0.0	56.7±11.5
PI-5	100±0.0	33.3±4.7	100.0±0.0	76.7±5.8
PI-6	100±0.0	50.0±16.3	100.0±0.0	93.3±5.8
PI-7	100±0.0	46.7±9.4	100.0±0.0	70.0±0.0
PI-8	80±10.0	50.0±14.1	100.0±0.0	66.7±5.8
PI-9	100±0.0	53.3±4.7	100.0±0.0	93.3±5.8
PI-10	100±0.0	56.7±4.7	100.0±0.0	90.0±10.0
PI-11	100±0.0	46.7±4.7	100.0±0.0	80.0±10.0
PI-12	100±0.0	40.0±8.1	100.0±0.0	60.0±10.0
PI-13	100±0.0	70.0±8.1	100.0±0.0	93.3±5.8
PI-14	100±0.0	56.7±4.7	100.0±0.0	66.7±11.5
PI-15	100±0.0	40.0±8.1	100.0±0.0	66.7±5.8
PI-16	100±0.0	73.3±4.7	100.0±0.0	100.0±0.0
PI-17	100±0.0	66.7±4.7	100.0±0.0	70.0±10.0
Hexaflumuron	100±0.0	66.7±4.7	100.0±0.0	83.3±11.5

Data are mortality±SD (*n*=3).

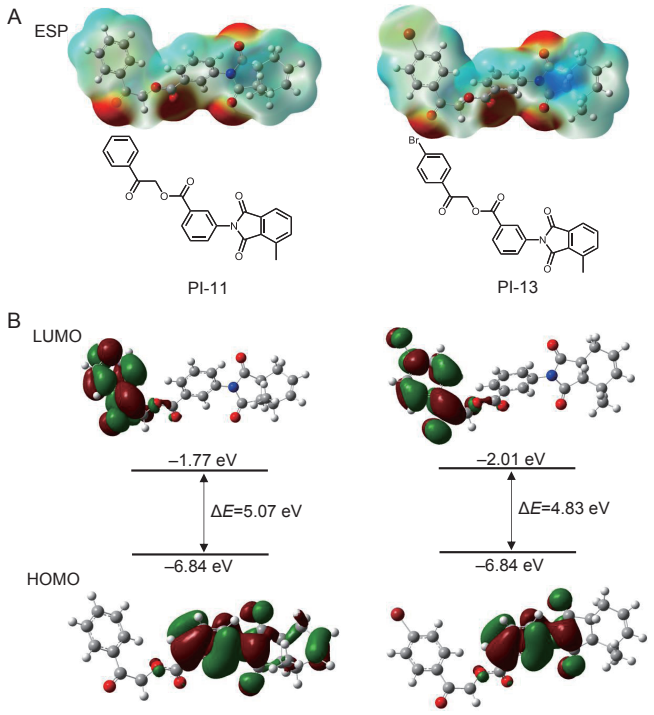


Fig. 5 The electrostatic potential distributions (ESP) and density functional theory (DFT) calculation analyses of PI-11 and PI-13. A, ESP of **PI-11** and **PI-13**. B, the energy difference Δ*E* between the lowest unoccupied molecular orbital (LUMO) and the highest occupied molecular orbital (HOMO) of **PI-11** and **PI-13** *via* DFT calculation.

distribute in its *p*-bromophenyl side chain and the **PI** fragment excluding the cyclohexene moiety, respectively. These computational findings suggest that **PI-13**, with its smaller energy gaps, exhibits enhanced insecticidal and enzyme inhibitory activity, aligning with experimental results. This research provides valuable guidance for future derivatization of **PI**-series compounds. For example, incorporating electron-withdrawing groups at the 3- or 4-position of the benzoyl benzene ring can expand the negative charge region through inductive effects, improving electrostatic complementarity with the target enzyme's active site. Alternatively, substituting the benzoyl benzene ring with nitrogen- or sulfur-containing heterocycles may utilize conjugative effects to reduce the HOMO-LUMO energy gap, potentially enhancing binding affinity and biological efficacy.

3.8. Toxicity of PI-series compounds to natural enemy *T. ostriniae*

The development of green pesticides necessitates ensuring safety for natural enemies, a critical factor in maintaining ecological balance while managing pest populations effectively. Among these natural enemies, *T. ostriniae* represents a particularly effective antagonist against *O. furnacalis*. This parasitic wasp specifically targets *O. furnacalis* eggs, effectively limiting pest population growth at its initial stage. This study evaluated the safety of **PI**-series compounds against *T. ostriniae* using egg dipping and insecticide film methods. As demonstrated in Table 4, the egg dipping method indicated that representative **PI**-series compounds minimally affected the emergence probability of *T. ostriniae* progeny. The dry film method similarly confirmed the compounds' safety profile regarding *T. ostriniae*. Furthermore, these compounds exhibited reduced toxicity compared to hexaflumuron, suggesting their potential as safer alternatives in pest management strategies.

3.9. Biosafety prediction

In developing agrochemicals that balance effectiveness with environmental safety, evaluating potential risks to non-target organisms remains crucial. As shown in Table 5, all target compounds demonstrated negative predictions for carcinogenicity, honey bee toxicity, and oral toxicity in rats. These findings suggest favorable safety profiles regarding both mammals and honey bees. Subsequent research may validate these predictions through *in vivo* experiments to confirm the application potential of these compounds in agricultural settings.

4. Discussion

4.1. Virtual screening: An accelerator for targeted lead discovery

Virtual screening in this study demonstrates its effectiveness as a cost-efficient and time-saving approach for identifying novel enzyme inhibitors (Hu *et al*. 2017). Through the implementation of a parallel docking strategy targeting chitinase O*f*Chi-h, the **PI** scaffold emerged as a promising candidate structure. This methodology eliminated the resource-intensive trial-and-error process characteristic of traditional pesticide development, aligning with contemporary approaches in data-driven drug discovery. Compound **PI-1** emerged as a novel O*f*Chi-h inhibitor with an IC_{50} value of 10.7 μmol L^{-1}. These findings demonstrate both the efficacy of the virtual screening methodology and illustrate the progressive integration of computational simulation techniques with experimental biology, accelerating the development of environmentally sustainable insecticides.

4.2. *In vitro* and *in vivo* bioassay: The basis for obtaining potential candidates

The structural diversification of lead compound **PI-1** revealed specific SARs governing inhibitory potency against O*f*Chi-h. Systematic modifications of substituents at the R_1, R_2, R_3, and R_4 positions of the phenyl-isoindole-1,3-dione scaffold identified key activity determinants. Halogen substitution at the 4-position

Table 4 Toxicity of PI-series compounds against *Trichogramma ostriniae*

Compound	Survival/Emergence rate (%)	
	Dry-film	Soaking
PI-5	95.1±0.9	86.0±5.3
PI-10	95.6±3.3	83.9±9.1
PI-13	93.6±4.2	87.9±4.1
PI-16	90.7±8.9	87.1±3.3
PI-17	91.9±5.0	89.2±7.7
Hexaflumuron	88.1±1.5	82.4±7.4

Data are mean±SD (*n*=3).

Table 5 Carcinogenicity, honey bee toxicity, and oral toxicity prediction of PI-series compounds

Compound	Carcinogenicity	Honey bee toxicity	Rat oral toxicity	
			LD_{50} (mg kg^{-1})	Toxicity grade (US EPA)
PI-1	Negative	Low	–	–
PI-2	Negative	Low	876.63	Low
PI-3	Negative	Low	826.7	Low
PI-4	Negative	Low	947.39	Low
PI-5	Negative	Low	–	–
PI-6	Negative	Low	932.81	Low
PI-7	Negative	Low	1,037.38	Low
PI-8	Negative	Low	830.34	Low
PI-9	Negative	Low	721.37	Low
PI-10	Negative	Low	742.55	Low
PI-11	Negative	Low	950.02	Low
PI-12	Negative	Low	948.15	Low
PI-13	Negative	Low	808.13	Low
PI-14	Negative	Low	1,045.82	Low
PI-15	Negative	Low	621.72	Low
PI-16	Negative	Low	–	–
PI-17	Negative	Low	–	–

– indicates no value was obtained through the toxicity estimation software tool, an open-source toxicity prediction resource.

of the benzene ring (R_1) exhibited a size-dependent effect: bromine (**PI-3**, IC_{50}=7.3 μmol L^{-1}) showed greater efficacy than chlorine (**PI-1**, IC_{50}=10.7 μmol L^{-1}) and fluorine (**PI-2**) substituents. Electron-withdrawing groups at the 3-position of R_1 (e.g., nitro in **PI-5**) demonstrated superior performance compared to electron-donating groups (e.g., methoxy in **PI-6**), potentially due to enhanced electrostatic complementarity with positively charged residues in O*f*Chi-h. Methyl substitution at R_3 (**PI-10**, IC_{50}=3.8 μmol L^{-1}) enhanced potency, potentially by optimizing the scaffold's conformation for enzyme binding. Based on these SARs, subsequent optimization maintained the R_3 methyl group while exploring R_1 substitutions. Electron-withdrawing groups at the 4-position of R_1 (e.g., bromine in **PI-13**, IC_{50}=2.6 μmol L^{-1}) consistently demonstrated superior performance compared to electron-donating groups (e.g., methyl in **PI-12**), while 3-nitro substitution (**PI-16**, **PI-17**) further enhanced potency. These findings demonstrate the synergistic effect of halogen/electron-withdrawing substituents at R_1 and hydrophobic moieties at R_3 in optimizing binding to O*f*Chi-h. The *in vitro* inhibitory activity results establish a foundation for future compound derivatization.

The *in vivo* bioassay results confirm the *in vitro* findings and demonstrate the practical potential of **PI**-series compounds as insecticides (Zhang *et al.* 2021). The significant mortality rates observed in *O. furnacalis* and *P. xylostella* at both 500 and 200 mg L^{-1} concentrations indicate effective disruption of lepidopteran pest physiological processes. Compounds with potent O*f*Chi-h inhibitory activity (e.g., **PI-13** and **PI-17**) demonstrated enhanced efficacy against *O. furnacalis* compared to the control drug hexaflumuron, suggesting a novel mechanism targeting insect molting processes. The development of compounds with new modes of action holds particular significance for sustainable pest management, given increasing pest resistance to conventional insecticides (Ding *et al.* 2025).

4.3. Mechanism of action: Structural and electronic insights

The profound impact of **PI-13** and **PI-17** on *O. furnacalis* larval development manifested through significant reductions in body weight (27–33%) and length (22–23%) after 6 days of exposure at 10 μmol L^{-1} (Fig. 4-A and B). SEM revealed direct structural evidence of cuticular damage induced by **PI**-series compounds (Fig. 4-D). Compared to the smooth, uniformly structured cuticle of control larvae, the inhibitor-treated larvae demonstrated pronounced morphological aberrations, including irregular wrinkles, protruding chitin particles, and a compact yet disorganized arrangement of cuticular components. These alterations likely stem from the inhibition of O*f*Chi-h, which plays an essential role in degrading the chitin matrix during apolysis (the separation of the old cuticle from the epidermis). Without functional chitinase activity, the old cuticle cannot undergo proper recycling, resulting in incomplete molting, mechanical weakness in the exoskeleton, and ultimately, developmental arrest or mortality. The correlation between enzyme inhibition and cuticular defects establishes O*f*Chi-h as the primary molecular target of **PI**-series compounds. Given the absence of chitin in mammalian and plant systems, this insect-specific mechanism of action provides **PI**-series compounds with potential as environmentally friendly insecticides (Ding *et al.* 2025). Furthermore, the morphological and behavioral endpoints observed here establish a robust foundation for further mechanistic investigations.

ESP and DFT analyses elucidated the molecular basis of **PI**-series compounds' activity (Song *et al.* 2025). The bromine substitution in **PI-13** generated localized negative charge clusters, enhancing interactions with positively charged amino acids in the O*f*Chi-h active site. Additionally, DFT revealed that the smaller HOMO-LUMO energy gap (ΔE) of **PI-13** enabled more efficient electron transfer with the enzyme, correlating with its higher bioactivity. These calculation results illuminate the SARs of **PI**-series compounds and provide valuable guidance for their further derivatization. For instance, introducing electron-withdrawing groups such as nitro or cyano at the 3-position of the benzene ring, combined with halogens like fluorine or bromine at the 4-position, can enhance the negative charge region through the inductive effect, thereby improving electrostatic complementarity with the enzyme's active site. Alternatively, substituting the benzene ring with sulfur-containing heterocycles (e.g., thiophene or thiazole) can further reduce the energy gap *via* conjugation effects, enhancing binding affinity to *Of*Chi-h.

4.4. Biosafety: A critical step toward sustainable pest management

The environmental safety of **PI**-series compounds constituted a central focus of this study. Bioassays with the natural enemy *T. ostriniae*, a key biocontrol agent in maize ecosystems, demonstrated negligible toxicity, as neither egg-dipping nor dry-film exposure methods significantly affected wasp progeny emergence (Zhou *et al.* 2024). This contrasts markedly with conventional insecticides such as hexaflumuron, which frequently demonstrate adverse effects

on non-target arthropods. Moreover, toxicity predictions for mammals and bees (e.g., negative carcinogenicity, mutagenicity, and oral toxicity results) underscore the **PI**-scaffold's benign profile toward non-target organisms (Shen *et al*. 2024). These findings prove crucial for translating laboratory-based discoveries into field-applicable tools, as they align with increasing regulatory and societal demands for pesticides that maintain ecological equilibrium.

5. Conclusion

This study presents a virtual screening strategy to identify a novel **PI** scaffold targeting O*f*Chi-h. Through comprehensive investigations including structural similarity screening, enzyme inhibitory activity assays, SARs analysis, and molecular docking studies, compound **PI-17** was identified, demonstrating effective inhibitory activity with a K_i value of 2.3 μmol L^{-1} for O*f*Chi-h. The potent inhibitors **PI-13** and **PI-17** exhibited significant efficacy in suppressing the growth and development of *O. furnacalis* larvae. Analysis of the insecticidal activity of **PI**-series compounds revealed superior insecticidal potency against *O. furnacalis* and *P. xylostella* compared to the control drug hexaflumuron. ESP and DFT analyses indicated that bromine substitution in **PI-13** modified charge distribution and molecular orbital localization, resulting in a reduced HOMO-LUMO energy gap correlating with enhanced bioactivity. Additionally, **PI**-series compounds demonstrated high safety profiles for the natural enemy *T. ostriniae* and non-target organisms including honey bees and rats. This research establishes the **PI** as a novel scaffold for O*f*Chi-h inhibition, presenting significant potential for advancing environmentally friendly insecticides and sustainable pest control strategies.

Acknowledgements

We acknowledge the financial support by the National Natural Science Foundation of China (32472591), the Key Research and Development Project of Hebei Province, China (22326508D), the Talents Introduction Program in Hebei Agricultural University, China (YJ2021021), the Central Guide Local Science and Technology Development Fund Project of Hebei Province, China (236Z6506G).

Declaration of competing interest

The authors declare that they have no conflict of interest.

Declaration of generative AI and AI-assisted technologies in the writing process

The authors declare that they did not use AI in the preparation and writing of this manuscript.

Ethical statements

All applicable international, national and institutional guidelines for the care and use of animals were followed.

Appendix associated with this paper is available at https://doi.org/10.1016/j.jia.2025.08.019

References

Chen L, Liu T, Duan Y W, Lu X H, Yang Q. 2017. Microbial secondary metabolite, phlegmacin B1, as a novel inhibitor of insect chitinolytic enzymes. *Journal of Agricultural and Food Chemistry*, **65**, 3851–3857.

Chen L, Liu T, Zhou Y, Chen Q, Shen X, Yang Q. 2014. Structural characteristics of an insect group I chitinase, an enzyme indispensable to moulting. *Acta Crystallographica* (Section D: Structural Biology), **70**, 932–942.

Chen W, Yang Q. 2020. Development of novel pesticides targeting insect chitinases: A minireview and perspective. *Journal of Agricultural and Food Chemistry*, **68**, 4559–4565.

Cui H Y, Wang Y, Peng X, Wang Y T, Zhao Z W. 2020. Feeding effects of *ds*NPF interference in *Ostrinia furnacalis*. *Journal of Integrative Agriculture*, **19**, 1475–1481.

Deng J Y, Lan C Y H, Zhou J X, Yao Y B, Yin X H, Fu K Y, Ding X H, Guo W C, Liu W, Wang N, Wang F M. 2023. Analysis of sex pheromone production and field trapping of the Asian corn borer in Xinjiang, China. *Journal of Integrative Agriculture*, **22**, 1093–1103.

Ding B K, Ma S J, Yang M L, Zhang Q G, Hua X J, Zhang J H, Bai S M, Zhang L H, Dong J G, Shen S Q, Dong L L. 2025. Rational design of azo-aminopyrimidine derivatives as the potent lepidoptera-exclusive chitinase inhibitors. *Plant Biotechnology Journal*, **23**, 780–791.

Ding Y, Chen S Z, Liu H, Liu T, Yang Q. 2023a. Discovery of multitarget inhibitors against insect chitinolytic enzymes *via* machine learning-based virtual screening. *Journal of Agricultural and Food Chemistry*, **71**, 8769–8777.

Ding Y, Chen S Z, Zhang F, Li W D, Ge G B, Liu T, Yang Q. 2023b. Chitinase is a potent insecticidal molecular target of camptothecin and its derivatives. *Journal of Agricultural and Food Chemistry*, **71**, 1845–1851.

Dong L L, Shen S Q, Jiang X, Ding B K, Yang M L, Chen W, Liu Y X, Chen Z Y, Cao Q N, Gao Y M, Ma S J, Zhang L H, Dong J G, Yang Q. 2023. Identification of triazolo-quinazolinone derivatives as novel and potent chitinase *Of*Chi-h inhibitors based on structure-based virtual screening. *Journal of Agricultural and Food Chemistry*, **71**, 17410–17419.

Dong L L, Shen S Q, Xu Y F, Wang L, Yang Q, Zhang J J, Lu H Z. 2021. Identification of novel insect β-N-acetylhexosaminidase *Of*Hex1 inhibitors based on virtual screening, biological evaluation, and molecular dynamics simulation. *Journal of Biomolecular Structure and Dynamics*, **39**, 1735–1743.

Duan Y W, Liu T, Zhou Y, Dou T Y, Yang Q. 2018. Glycoside hydrolase family 18 and 20 enzymes are novel targets of the traditional medicine berberine. *Journal of Biological Chemistry*, **293**, 15429–15438.

Ece A. 2023. Computer-aided drug design. *BMC Chemistry*, **17**, 3.

Fan Z Z, Song Y F, Zhao S Y, Wu K M. 2024. Invasion of fall armyworm led to the succession of maize pests in Southwest China. *Journal of Integrative Agriculture*, **23**, 1300–1314.

Ge W C, Qiao S T, Liu C, Guo F R, Wang S, Sun H, Liu Y, Yang F X, Wu S F, Gao C F. 2025. Baseline establishment, susceptibility monitoring and risk assessment of cyproflanilide, a novel meta-diamide insecticide, against *Chilo suppressalis* (Lepidoptera: Crambidae) in China. *Journal of Integrative Agriculture*, **24**, 4342–4354.

Guo J F, He K L, Meng Y J, Hellmich R, Chen S J, Lopez M D, Lauter N, Wang Z Y. 2022. Asian corn borer damage is affected by rind penetration strength of corn stalks in a spatiotemporally dependent manner. *Plant Direct*, **6**, 10.

Han Q, Wu N, Liu Y Y, Zhang J Y, Zhang R L, Li H L, Jiang Z Y, Huang J X, Duan H X, Yang Q. 2022. Piperonyl-tethered rhodanine derivatives potently inhibit chitinolytic enzymes of *Ostrinia furnacalis*. *Journal of Agricultural and Food Chemistry*, **70**, 7387–7399.

Han Q, Wu N, Zhang J Y, Feng T Y, Zi Y J, Zhang R L, Zou R X, Liu Y Y, Yang Q, Duan H X. 2023. Discovery of rhodanine inhibitors targeting *Of*ChtI based on the π-stacking effect and aqueous solubility. *Journal of Agricultural and Food Chemistry*, **71**, 18685–18695.

Hu H B, Xia J, Wang D M, Wang X S, Wu S. 2017. A thoroughly validated virtual screening strategy for discovery of novel HDAC3 inhibitors. *International Journal of Molecular Sciences*, **18**, 137.

Jiang X, Kumar A, Motomura Y, Liu T, Zhou Y, Moro K, Zhang K Y J, Yang Q. 2020. A series of compounds bearing a dipyrido-pyrimidine

scaffold acting as novel human and insect pest chitinase inhibitors. *Journal of Medicinal Chemistry*, **63**, 987–1001.
Li L K, Duan R C, Li R Z, Zou Y, Liu J W, Chen F J, Xing G N. 2022. Impacts of corn intercropping with soybean, peanut and millet through different planting patterns on population dynamics and community diversity of insects under fertilizer reduction. *Frontiers in Plant Science*, **13**, 17.
Li W Q, Ding Y, Qi H T, Liu T, Yang Q. 2021. Discovery of natural products as multitarget inhibitors of insect chitinolytic enzymes through high-throughput screening. *Journal of Agricultural and Food Chemistry*, **69**, 10830–10837.
Liang P B, Li J Y, Chen W, Zhou H, Lai X N, Li J M, Xu Z Y, Yang Q, Zhang J J. 2024. Design of inhibitors targeting chitin-degrading enzymes by bioisostere substitutions and scaffold hopping for selective control of *Ostrinia furnacalis*. *Journal of Agricultural and Food Chemistry*, **72**, 10794–10804.
Liu T, Chen L, Zhou Y, Jiang X, Duan Y W, Yang Q. 2017. Structure, catalysis, and inhibition of *Of*Chi-h, the lepidoptera-exclusive insect chitinase. *Journal of Biological Chemistry*, **292**, 2080–2088.
Luo L L, Chang Q R, Wang Q, Huang Y. 2021. Identification and severity monitoring of maize dwarf mosaic virus infection based on hyperspectral measurements. *Remote Sensing*, **13**, 19.
Lu Q, Xu L P, Liu L, Zhou Y, Liu T, Song Y X, Ju J H, Yang Q. 2021. Lynamicin B is a potential pesticide by acting as a lepidoptera-exclusive chitinase inhibitor. *Journal of Agricultural and Food Chemistry*, **69**, 14086–14091.
Maddeboina K, Yada B, Kumari S, McHale C, Pal D, Durden D L. 2024. Recent advances in multitarget-directed ligands *via* in silico drug discovery. *Drug Discovery Today*, **29**, 23.
Monjane A L, Dellicour S, Hartnady P, Oyeniran K A, Owor B E, Bezuidenhout M, Linderme D, Syed R A, Donaldson L, Murray S, Rybicki E P, Kvarnheden A, Yazdkhasti E, Lefeuvre P, Froissart R, Roumagnac P, Shepherd D N, Harkins G W, Suchard M A, Lemey P, *et al.* 2020. Symptom evolution following the emergence of maize streak virus. *eLife*, **9**, 19.
Niazi S K, Mariam Z. 2024. Computer-aided drug design and drug discovery: A prospective analysis. *Pharmaceuticals*, **17**, 22.
Perry E D, Moschini G. 2020. Neonicotinoids in US maize: Insecticide substitution effects and environmental risk. *Journal of Environmental Economics and Management*, **102**, 19.
Shen S Q, Ding B K, Yang M L, Zhang J H, Bai S M, Ma S J, Zhang L H, Dong J G, Dong L L. 2024. Modification of azo-aminopyrimidines as potent multitarget inhibitors of insect chitinolytic enzymes *Of*Chi-h and *Of*Hex1. *Journal of Agricultural and Food Chemistry*, **72**, 26957–26966.
Shen S Q, Dong L L, Chen W, Wu R J, Lu H Z, Yang Q, Zhang J J. 2019. Synthesis, optimization, and evaluation of glycosylated naphthalimide derivatives as efficient and selective insect β-N-acetylhexosaminidase *Of*Hex1 inhibitors. *Journal of Agricultural and Food Chemistry*, **67**, 6387–6396.
Song X M, Wang H J, Zou W, Hong H, Gao Y C, Zhao C, Xu H H, Yao G K. 2025. New isoxazoline cyclopropyl-picolinamide derivatives as potential insecticides. *Journal of Agricultural and Food Chemistry*, **73**, 6589–6598.
Sun C X, Li S J, Wang K, Yin X M, Wang Y M, Du M F, Wei J Z, An S H. 2022. Cyclosporin A as a potential insecticide to control the Asian corn borer *Ostrinia furnacalis* guenee (lepidoptera: pyralidae). *Insects*, **13**, 13.
Taddele A, Azerefegne F, Beyene Y. 2023. Crop injury and yield losses in maize by the African maize stem borer, *Busseola fusca* (fuller) (lepidoptera: noctuidae) in Southern Ethiopia. *International Journal of Pest Management*, **69**, 120–129.
Wang Y, Hou Y Y, Iqbal A, Wang S, Monticelli L S, Desneux N, Zang L S. 2024. Inundative release of Trichogramma dendrolimi at different developmental stages enhances the control efficacy over *Ostrinia furnacalis*. *Journal of Pest Science*, **97**, 1889–1898.
Wang Y C, Yang X D, Lin Y P, Cao Y, Chi D F. 2023. Studies on the degradation effect of corn straw by Asian corn borer larva (*Ostrinia furnacalis*) digestive enzymes combined with white rot fungus (*Phanerochaetc chrysosporium*). *3 Biotech*, **13**, 9.
Yang H B, Qi H T, Hao Z S, Shao X S, Liu T, Yang Q, Qian X H. 2020. Thiazolylhydrazone dervatives as inhibitors for insect N-acetyl-β-D-hexosaminidase and chitinase. *Chinese Chemical Letters*, **31**, 1271–1275.
Zhang X J, Yuan J B, Li F H, Xiang J H. 2021. Chitin synthesis and degradation in crustaceans: A genomic view and application. *Marine Drugs*, **19**, 23.
Zhang Y L, Zhang Y T, Fu M J, Yin G H, Sayre R T, Pennerman K K, Yang F S. 2018. RNA interference to control Asian corn borer using *ds*RNA from a novel glutathione-*S*-transferase gene of *Ostrinia furnacalis* (Lepidoptera: Crambidae). *Journal of Insect Science*, **18**, 9.
Zhao Z X, Chen W, Wang S M, Dong Y H, Yang Q, Zhang J J. 2023. Rational design of N-Methylcarbamoylguanidinyl derivatives as highly potent dual-target chitin hydrolase inhibitors for retarding growth of pest insects. *Journal of Agricultural and Food Chemistry*, **71**, 2817–2826.
Zhou W T, Arcot Y, Medina R F, Bernal J, Cisneros-Zevallos L, Akbulut M E S. 2024. Integrated pest management: An update on the sustainability approach to crop protection. *ACS Omega*, **9**, 41130–41147.
Zou R X, Li X, Jiang X, Shi D M, Han Q, Duan H X, Yang Q. 2024. Novel butenolide derivatives as dual-chitinase inhibitors to arrest the growth and development of the Asian corn borer. *Journal of Agricultural and Food Chemistry*, **72**, 5036–5046.
Zou X, Chen J Q, Duan Y W, Zhu W X, Yang Q. 2025. Twinstar is a chitin synthase interacting protein with an essential role in insect cuticle biosynthesis. *Journal of Integrative Agriculture*, **24**, 209–219.

Executive Editor-in-Chief Fanghao Wan
Managing Editor Lujuan Sun